Type II inhibitors targeting CDK2

Leila T. Alexander [§,‡,†], Henrik Möbitz [‖], Peter Drueckes [‖], Pavel Savitsky [§], Oleg Fedorov [§⊥], Jonathan M. Elkins [§⊥], Charlotte M. Deane [‡], Sandra W. Cowan-Jacob [‖], and Stefan Knapp [§&⊥*]

[§]Structural Genomics Consortium, University of Oxford, Old Road Campus Research Building, Roosevelt Drive, Oxford, OX3 7DQ, United Kingdom.

[‡]Department of Statistics, University of Oxford, 1 South Parks Road, Oxford, OX1 3TG, UK.

[‖]Novartis Institutes of Biomedical Research, Basel, Switzerland, Novartis Pharma AG, Postfach, CH-4002 Basel, Switzerland.

[⊥]Target Discovery Institute, University of Oxford, NDM Research Building, Roosevelt Drive, Oxford, OX3 7FZ, UK.

[&]Institute for Pharmaceutical Chemistry, Johann Wolfgang Goethe-University, Max-von-Laue-Str. 9, D-60438 Frankfurt am Main, Germany.

KEYWORDS Kinase, CDK2, type II inhibitor, DFG-out, conformation.

ABSTRACT: Kinases can switch between active and inactive conformations of the ATP/Mg^{2+} binding motif DFG which has been explored for the development of type I or type II inhibitors. However, factors modulating DFG conformations remain poorly understood. We chose CDK2 as a model system to study the DFG in-out transition on a target that was thought to have an inaccessible DFG-out conformation. We used site-directed mutagenesis of key residues identified in structural comparisons in conjunction with biochemical and biophysical characterization of the generated mutants. As a result, we identified key residues that facilitate the DFG-out movement, facilitating binding of type II inhibitors. However, surprisingly we also found that wild type CDK2 is able to bind type II inhibitors. Using protein crystallography structural analysis of the CDK2 complex with an aminopyrimidine-phenyl urea inhibitor (K03861) revealed a canonical type II binding mode and the first available type II inhibitor CDK2 co-crystal structure. We found that the identified type II inhibitors compete with binding of activating cyclins. In addition, analysis of the binding kinetics of the identified inhibitors revealed slow off-rates. The study highlights the importance of residues that may be distant to the ATP binding pocket in modulating the energetics of the DFG-out transition and hence inhibitor binding. The presented data also provide the foundation for a new class of slow off-rate cyclin-competitive CDK2 inhibitors targeting the inactive DFG-out state of this important kinase target.

The kinase catalytic domain is highly dynamic resulting in a number of conformations that can be targeted by small molecule inhibitors. The main binding modes have been classified as type I (inhibitors binding to the active kinase conformation), type II (inhibitors targeting an inactive conformation as a result of an outward flip of the conserved tripeptide motif DFG), and allosteric binding modes distal to the ATP binding site (type III and type IV) [1, 2]. In addition, alternative induced binding pockets adjacent to the ATP binding site may be explored as exemplified for recently developed highly specific ERK1/2 inhibitors [3].

The type II binding mode is by far the most explored inactive conformation to date. The DFG motif is a highly conserved metal binding motif that coordinates the ATP phosphate moieties in the catalytically active ATP bound state. The DFG motif can be dislodged resulting in the generation of a large binding pocket that accommodates inhibitors that fill the Phe side chain pocket vacated by the DFG motif (type II inhibitors). Due to the larger diversity of the DFG-out binding pocket and the more dynamic nature of the DFG-out inactive states, this binding mode has generated considerable interest [1] and gave rise to speculations that type II inhibitors may have favorable selectivity when compared to type I inhibitors [4].

The DFG-out conformation was first observed in the apo-crystal structure of the kinase domain of the human insulin receptor [5] but the importance of this binding

pocket has only been realized after the kinase inhibitor imatinib was co-crystallized with Abl [6]. Type II inhibitors are often anchored to the DFG-out pocket via hydrogen bonds to the conserved αC glutamate (αC-Glu) and the aspartate of the DFG (DFG-Asp) motif resulting in the definition of a type II inhibitor specific pharmacophore [1].

Which kinases can be targeted with type II inhibitors is still an open question. Early work on type II inhibitor development suggested that the type II binding mode might be favoured by smaller gatekeeper residues [7] but kinases with bulkier gatekeeper residues have also been shown to bind type II inhibitors in the DFG-out conformation [8, 9]. A recent survey of all available kinase crystal structures revealed that there is no preference for smaller gatekeeper residues [2]. However, this observation cannot rule out the possibility that smaller gatekeeper residues still favor the DFG-out conformation energetically as mutation into larger gatekeeper residues often leads to kinase activation in cancer and as a consequence stabilization of the active state [10-14]. Thus, the structural mechanisms that favour the DFG-out conformation are still poorly understood. Some kinases such as the insulin receptor, FLT3 or the cyclin dependent kinase CDK6 seem to spontaneously assume DFG-out conformations even in the absence of type II inhibitors [5, 15] while other kinases that can be targeted by type II inhibitors adopt a DFG-in conformation in crystal structures of the inactive, un-phosphorylated kinase in the absence of inhibitors[16]. Molecular dynamics studies suggested that for the Abl tyrosine kinase the DFG-out conformation is pH-dependent [17]. Comparison of recent crystal structures of Aurora kinase inhibitor complexes showed that inhibitors that alter charge distribution in the proximity of the DFG backbone may induce a DFG-out flip [18]. Site-directed mutagenesis studies showed that both the gatekeeper and the residue located N-terminal to the DFG motif have a critical role in determining the propensity of the DFG-out conformation [19]. Using a small library of promiscuous type II inhibitors, Zhao et al demonstrated that at least 200 kinases can bind type II inhibitors, suggesting that type II inhibitors may not be intrinsically more selective than type I inhibitors [2]. However, a type II binding mode will not be seen for all kinases bound to a type II inhibitor [20] and a number of intermediate states of the DFG-in and DFG-out conformations are frequently observed in kinase inhibitor complexes, highlighting the complexity of this inactive state. For example, the crystal structure of the typical type I inhibitor dasatinib binds to BTK in an intermediate state of the DFG motif [21]. Experimental determination of the binding mode of type II inhibitors is therefore essential.

Here we analysed the influence of key residues determining the energetics of the DFG-out conformation using CDK2 as a model. For many years CDK2 has been regarded as an attractive drug target because deregulation of CDK2 is frequently associated with cancer. For these reasons, extensive effort from both pharmaceutical industry and academic groups lead to the development of hundreds of small-molecule CDK2 inhibitors, several of which have reached phase III clinical trials as anti-tumor agents [22]. The considerable interest in CDK2 resulted in many co-crystal structures making CDK2 the kinase with the highest number of PDB depositions (see **Supplemental Figure 1**). Interestingly, despite the large number of structural data, no DFG-out conformation has yet been observed.

Using site-directed mutagenesis, we increased the propensity of CDK2 to bind type II inhibitors. Surprisingly, we also found that wild type CDK2 can assume a DFG-out conformation and determined the first crystal structure showing a DFG-out binding mode for this well studied protein kinase. Type II inhibitor binding competed with activation of CDK2 by cyclins, suggesting that inactive CDK can be locked by type II inhibitors in a conformation that is not competent for cyclin binding, preventing activation of this kinase. In addition, the studied CDK2 type II inhibitors showed slow off-rates enabling development of inhibitors with prolonged target engagement. The data presented here will enable the development of optimized type II CDK2 inhibitors with slow off-rate binding kinetics and introduces an alternative strategy for targeting CDK2 in its inactive state.

RESULTS

At the time of writing, CDK2 had the largest number of kinase structures in the PDB (**Supplemental Figure 1**) with no DFG-out conformation having been observed. This provided an excellent reference state for a mutagenesis study of a kinase that would presumably only bind type I inhibitors. By mutating amino-acids that may influence DFG movement, our goal was to get insight on key interactions that facilitate the DFG-out movements.

Following a recent large scale sequence and structural comparison of the human kinome [23], we focused our attention on the three key positions. The first is the gatekeeper residue (F80 in CDK2). The size of the gatekeeper side chain has been recognized to control the accessibility to the deeper hydrophobic pocket at the back of the ATP-binding site and controls kinase selectivity for ATP-competitive inhibitors [21, 24]. Sequence analysis revealed that kinases with threonine or methionine at the gatekeeper position favor DFG-out conformations, whereas phenylalanine, leucine or valine gatekeeper residues are less likely to assume a DFG-out conformation. Therefore we mutated F80 to threonine or methionine (F80T and F80M).

The second position for point mutations was cysteine 118 located on the αE helix (**Figure 1a**). We observed that in CDK2 the DFG-Phe146 is 'sandwiched' between the large gatekeeper (F80) and C118. The side chain of C118 is at a distance of 3.8Å from the aromatic ring of the DFG-Phe (closest atom to atom contact) and complies with the geometry known to form a strong sulphur-arene interaction in protein structures (**Figure 1b**) [25, 26].

At the time of our sequence and structure analysis, the only non-tyrosine kinases with available structures of a DFG-out conformation were p38α, Aurora A, CDK6 and CDK7. Sequence alignment of nine CDK family members

indicated that both CDK6 and CDK7 had leucine at the position of C118 (**Figure 1c**). Interestingly, about 90% of tyrosine kinases, which account for the vast majority of available DFG-out structures, also have leucine at this position. All these observations resulted in the hypothesis that the interaction of C118 with F146 stabilizes the DFG motif in an active 'in' conformation. Cysteine 118 was therefore mutated to leucine (C118L) to remove the sulphur-aromatic interaction and allow for rotation of the DFG-Phe into the ATP-binding pocket, and to isoleucine to investigate the effect of this residue on αC-helix displacement.

The third position for point mutations was the residue preceding the DFG motif (termed DFG-1). This residue often makes direct contacts with the bound ligand and similar to the gatekeeper, stabilizes the regulatory hydrophobic spine [27]. While alanine is the most commonly observed residue across the kinome in this position, glycine and cysteine appear to play a role in lowering the torsional barrier for the DFG backbone rotation. To test the role of this residue we mutated the DFG-1 position to cysteine (A144C) and glycine (A114G) followed by generation of double mutants (C118L/A144C and C118L/A144G) to combine the hypothesized DFG-out stabilizing effects.

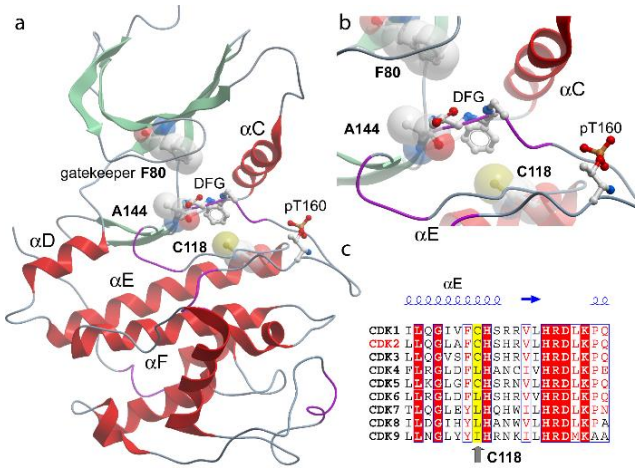

Figure 1. Location of CDK2 residues targeted by mutagenesis: (a) Structure of CDK2 (PDB: 1qmz) shown as a ribbon diagram with mutated residues highlighted in bold and important structural elements are labelled. (b) Detailed view of the DFG motif. (c) Sequence alignment of nine human CDK family members. The position corresponding to C118 of CDK2 located on the αE helix is highlighted in yellow and by a grey arrow.

Structural integrity and stability of mutants

The effect of the mutations on the structural integrity and thermal stability of CDK2 was investigated by measuring the temperature at which the protein unfolds (melting temperature, T_m). The wild-type enzyme exhibited a melting temperature of 52.4 ± 0.5 °C (**Table 1**). Overall, the mutants demonstrated similar stability with melting temperatures ranging from 48 °C to 55 °C, confirming that the introduced mutations had no strong effect on protein stability. It is interesting to note, that the average T_m of the A144C mutant was about 4 °C lower (48.0 ± 0.3 °C. This destabilization is compensated when a second point mutation is introduced. The C118L/A144C and C118L/A144G double mutants had similar melting temperatures to the wild-type (51.8 ± 0.2 °C and 53.0 ± 0.2 °C respectively).

Table 1. Melting temperatures (T_m) obtained for the wild-type CDK2 and mutants. Mean values and standard deviations were derived from at least 40 replicates.

Protein	T_m (°C)
Wild-type	52.4 ± 0.5
F80T	54.3 ± 0.2
F80M	52.3 ± 0.3
C118L	55.1 ± 0.3
C118I	54.0 ± 0.2
A144C	48.0 ± 0.3
A144G	50.6 ± 0.2
C118L/A144C	51.8 ± 0.2
C118L/A144G	53.0 ± 0.2

Effect of mutations on CDK2 enzymatic activity

Peptide titration experiments resulted in similar K_m (peptide) values for all CDK2 mutants, indicating that the mutations did not affect peptide binding. However, K_m^{ATP} values were observed to be increased for all mutants suggesting that inactivating mutations reduced affinity for ATP. Comparison of the catalytic rates (k_{cat}) revealed that the ability of the mutants to phosphorylate substrate was decreased (**Table 2**). The activity of the C118I mutant was decreased 10 times compared to the wild-type enzyme, while the F80M, C118L and A144G mutants demonstrated a nearly 70-fold decrease.

CDK2 can bind type II inhibitors in the absence of cyclin

We used temperature shift assays to probe the binding of both type I as well as type II inhibitors to wild type CDK2 as well as to the mutants. Interestingly, several type II inhibitors bound to the wild type CDK2 (**Figure 2**).

A significant increase in ΔT_m indicated higher affinity of type II compounds for the mutants C118L, A144C, and C118L/A144C (**Figure 3**). Next we used isothermal titration calorimetry (ITC) to measure the binding of the identified inhibitors in solution. ITC titrations of the CDK2 C118L/A144C mutant into the putative type II inhibitor **1** (K03861a) resulted in a K_d of 8.2 nM, while the single CDK2 point mutants C118L and A144C showed slightly weaker binding.

Table 2. Steady-state kinetic constants for the ATP titration experiments determined using Caliper microfluidic mobility shift assay.

CDK2 variant	Kinase concentration (nM)	K_m (μM)	k_{cat} (s^{-1})	k_{cat}/K_m (M^{-1} s^{-1} x 10^4)
WT	20	44.0 ± 14.5	18.1 ± 5.5	41.2 ± 18.5
F80T	100	Not converged*		
F80M	100	432.2 ± 21.8	2.6 ± 0.4	0.6 ± 0.1
C118L	50	328.1 ± 76.8	1.9 ± 0.2	0.6 ± 0.1
C118I	100	96.1 ± 16.1	3.3 ± 1.9	3.5 ± 2.0
A144C	100	51.6 ± 13.3	9.8 ± 0.6	18.9 ± 5.0
A144G	100	302.0 ± 74.6	2.1 ± 0.6	0.7 ± 2.5
C118L/A144C	100	52.4 ± 16.5	1.6 ± 0.3	3.1 ± 1.2
C118L/A144G	100	Not converged*		
co-expressed WT	10	27.2 ± 19.3	40.8 ± 8.4	149.9 ± 110.7

*Curves were not fitted because the data did not converge to a plateau.

This supported our hypothesis that the combination of both mutants would synergistically promote type II binding (K_d values of 20.0 nM and 14.3 nM respectively). Surprisingly, strong binding was also detected for wild type CDK2 with a dissociation constant (K_d) of 52.7 nM (**Figure 4a** and **Supplemental Table 1**).

We were interested to see if CDK2 and its mutants would bind type II inhibitors in the presence of cyclin. Therefore we repeated the ITC experiments using CDK2-Cyclin B complexes titrated into **1**. No binding of the wild-type CDK2-Cyclin B complex was detected but the cyclin B complex of the C118L/A144C mutant bound the type II compound **1** with a K_d of 135.3 nM, which is about 16 fold reduced affinity compared to CDK2 without Cyclin (**Figure 4b**).

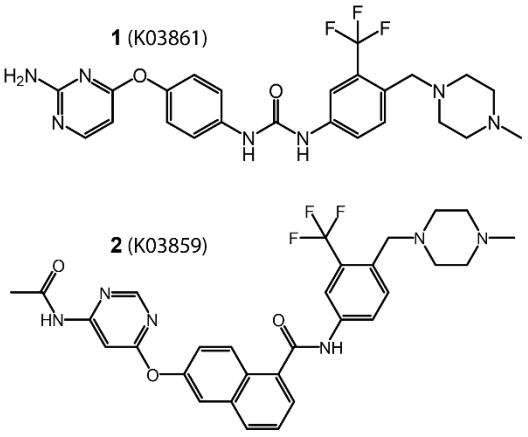

Figure 2. Chemical structures of the identified type II inhibitors.

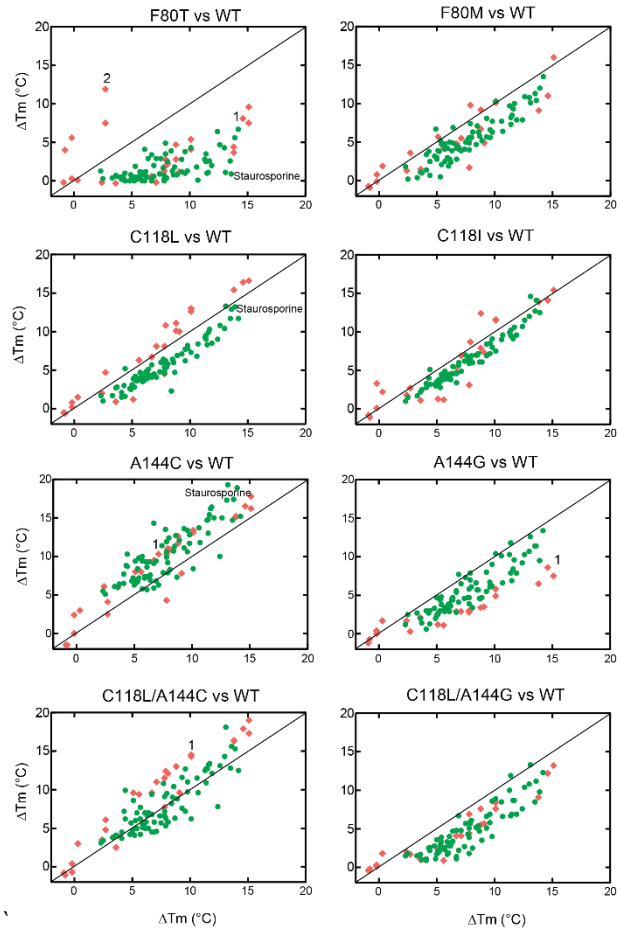

Figure 3. Scatter plots of relative compound binding for each CDK2 mutant with respect to the wild-type (WT) as established by temperature shift assays. Each value represents a ΔT_m in °C. Putative Type I inhibitors are shown as green circles and Type II inhibitors are shown as red rhombuses. Compounds of interest are labelled.

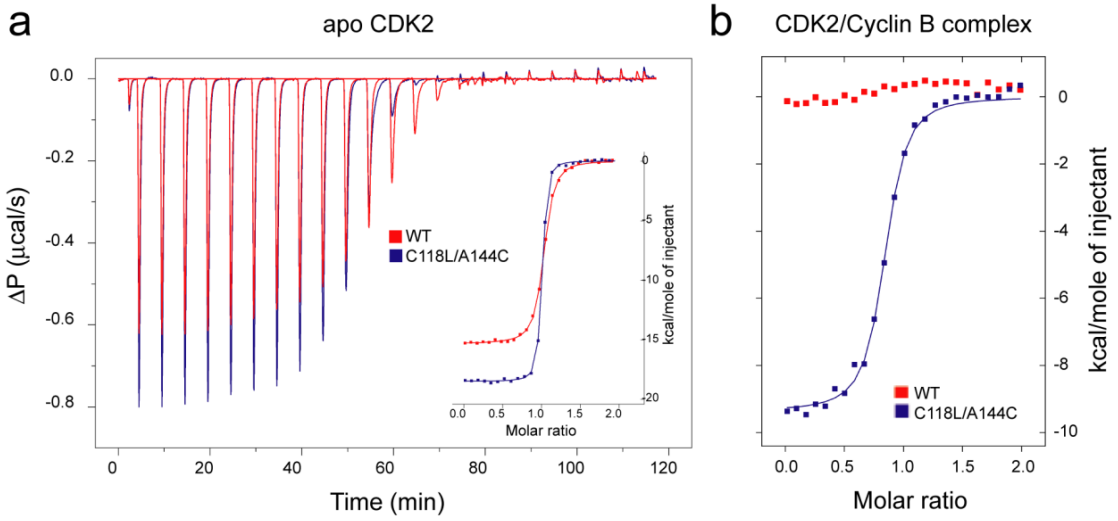

Figure 4. ITC experiments demonstrating binding of inhibitor 1 to wild-type CDK2 and to the C118L/A144C mutant. a) ITC data measured on apo-CDK2. Shown are raw heat effects of each injection as well as normalized binding heats (insert). Wild type CDK2 and the double mutant C118L/A144C are shown in red and blue respectively. b) ITC data measured on the CDK2-Cyclin B complex. Only normalized binding isotherms are shown. Solid lines represent a non-linear least squares fit to a single binding site model.

These findings indicate that the addition of cyclin made the DFG-out conformation inaccessible for type II binding in wild type CDK2, while the C118L/A144C mutant enabled binding due to its higher propensity to assume a DFG-out conformation.

In agreement with our ITC data, wild type CDK2 in complex with cyclin was not inhibited by type II inhibitors in enzyme kinetic assays up to an inhibitor concentration of 10 µM. In contrast, the mutants A144C and C118L/A144C showed considerable inhibition in the presence of type II inhibitors (see **Supplemental Table 2**).

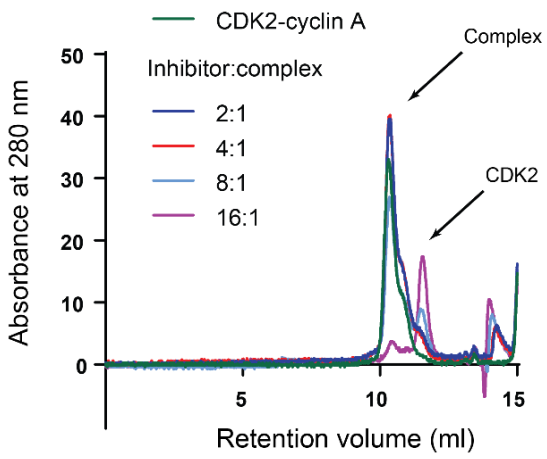

Figure 5. Size exclusion chromatography demonstrating that the type II inhibitor 1 displaces Cyclin A from the CDK2 complex. The CDK2-Cyclin A complex was incubated overnight with different ratios of inhibitor as indicated in the figure before the sample was analyzed on a size exclusion column.

The interaction of type II inhibitors with wild type CDK2 and the inhibition of this interaction by cyclin binding raised the question of whether type II inhibitors displace the cyclin or if the cyclin would still bind to an inactive CDK2 in the DFG-out conformation. To address this question we studied binding of Cyclin A to wild type CDK2 by size exclusion chromatography (SEC) in the presence of increasing concentration of the type II inhibitor **1** (**Figure 5**). The elution peaks of CDK2 and the CDK2-Cyclin A were identified using SEC runs in the absence of the inhibitor. Comparing SEC experiments with increasing inhibitor concentration revealed that Cyclin A dissociated from the kinase in a concentration-dependent manner suggesting that type II inhibitor binding leads to dissociation of the cyclin, further suggesting that the DFG-out binding mode is incompatible with cyclin binding.

Type II binding to CDK2 is associated with slow off-rates

Binding kinetics has developed into an important parameter during lead optimization as slow off-rate, which is characteristic for type II inhibitors, have been associated with better efficacy in cellular studies and potentially *in vivo* [28]. We therefore analyzed the binding kinetics of the identified type II inhibitors and found that the off-rate was slower for **1**, indicating that slow off-rate binding may be associated with the type II binding mode of this compound (**Figure 6**).

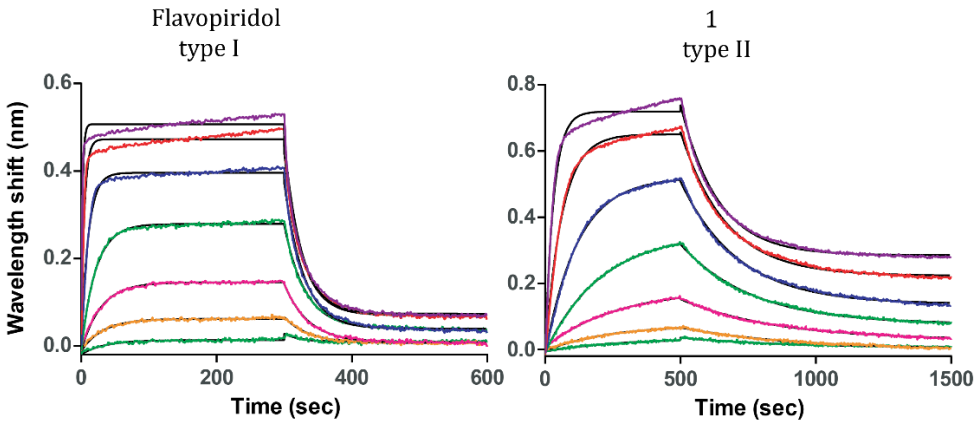

Figure 6. Biolayer interference (BLI) data measuring the binding kinetics of the type I inhibitor flavopiridol (a) and the type II inhibitor 1. The kinetic parameters derived from curve fitting were: flavopiridol : k_{on}: 5.0 10^4 (M^{-1} s^{-1}) k_{off}: 3.5 10^{-2} (s^{-1}); 1: k_{on}: 2.3 10^4 (M^{-1} s^{-1}) k_{off}: 3.2 10^{-3} (s^{-1})

Structure of wild type CDK2 in a DFG-out conformation

In order to confirm the type II binding mode of **1**, we determined the co-crystal structure of this inhibitor with CDK2 using X-ray crystallography. The resulting structure provided definitive evidence that CDK2 can adopt a DFG-out conformation, where DFG-Phe (F146) undergoes a large movement compared to all previous CDK2 crystal structures which exclusively revealed a DFG-in conformation (**Figure 7**).

Compound **1** occupied the adenine-binding pocket of the ATP-binding site and formed two hydrogen bonds within the hinge region: one between the pyramidine nitrogen and the backbone NH of L83, and the other between the amino group of the aminopyrimidine and the backbone carbonyl of L83. The carboxyl side-chain of the conserved αC-helix glutamate (E51) was engaged in at least one hydrogen bond interaction with the NH of the urea moiety, while maintaining the salt bridge with K33 and stabilizing an active 'αC-in' conformation. The carbonyl from the urea linker also accepted a hydrogen bond from the backbone NH of DFG-Asp (D145). Compound **1** contains a phenyl ring which is substituted with a trifluoromethyl group at the meta position. This typical type II scaffold motif projected into the hydrophobic pocket vacated by the rotation of the DFG-Phe side chain around the C-N bond of the DFG-Asp. There was a clear break in the electron density of the activation loop between residues 154-163 indicating that the activation loop was disordered as it has been often observed in inactive kinase structures.

A second molecule of **1** was found outside the ATP-binding pocket, packed between the C-lobe and αC-helix of the symmetry related molecule. Very similar examples with other protein kinases have been reported previously [29]. Because the ITC data indicated 1:1 stoichiometry of binding, we concluded that the **1** located outside the active site has no biological significance, and only serves to stabilize crystal contacts at the interface between symmetry-related molecules.

DISCUSSION AND CONCLUSIONS

This project tested the hypothesis that primary sequence alteration of a protein kinase can shift the conformational equilibrium between DFG-in and DFG-out states. CDK2 was chosen as a target that was thought to have an inaccessible DFG-out conformation due to the large conformational penalty between the 'in' and 'out' states and the lack of DFG-out inhibitor complexes despite the large number of experimental crystal structures. Key residues were identified by structural comparisons and were mutated to promote the DFG-out transition. Using temperature shift assays we identified a number of type II inhibitors that preferentially interacted with the mutants. However, binding of type II inhibitors to the wild-type CDK2 was also detected. The detailed characterization revealed that type II compounds were potent inhibitors of the monomeric CDK2, but not the CDK2 complex with cyclin. The co-crystal structure of CDK2 with type II inhibitor **1** confirmed the DFG-out binding mode. In the search for potent CDK2 inhibitors most inhibitor screens were probably carried out using the active cyclin-activated enzyme. Thus, due to the strong interaction of cyclin with CDK most type II inhibitors present in screening libraries have been missed. Interestingly, a recent study using the DiscoverX binding assay, which uses CDK2 without Cyclin, also identified type II inhibitors binding to CDK2 [2].

Additionally, we demonstrated that the large conformational changes required to accommodate type II inhibitor binding were responsible for slow binding kinetics. In particular this conformational adaptation plays a key role in stabilizing the compound-target complex, thereby increasing the compound residence time. While effectiveness of an inhibitor is traditionally quantified using K_d or IC_{50} values, which are related to the concentration of inhibitor needed for a certain level of target occupancy under equilibrium conditions, inhibitor-target binding *in vivo* is not wholly governed by equilibrium conditions.

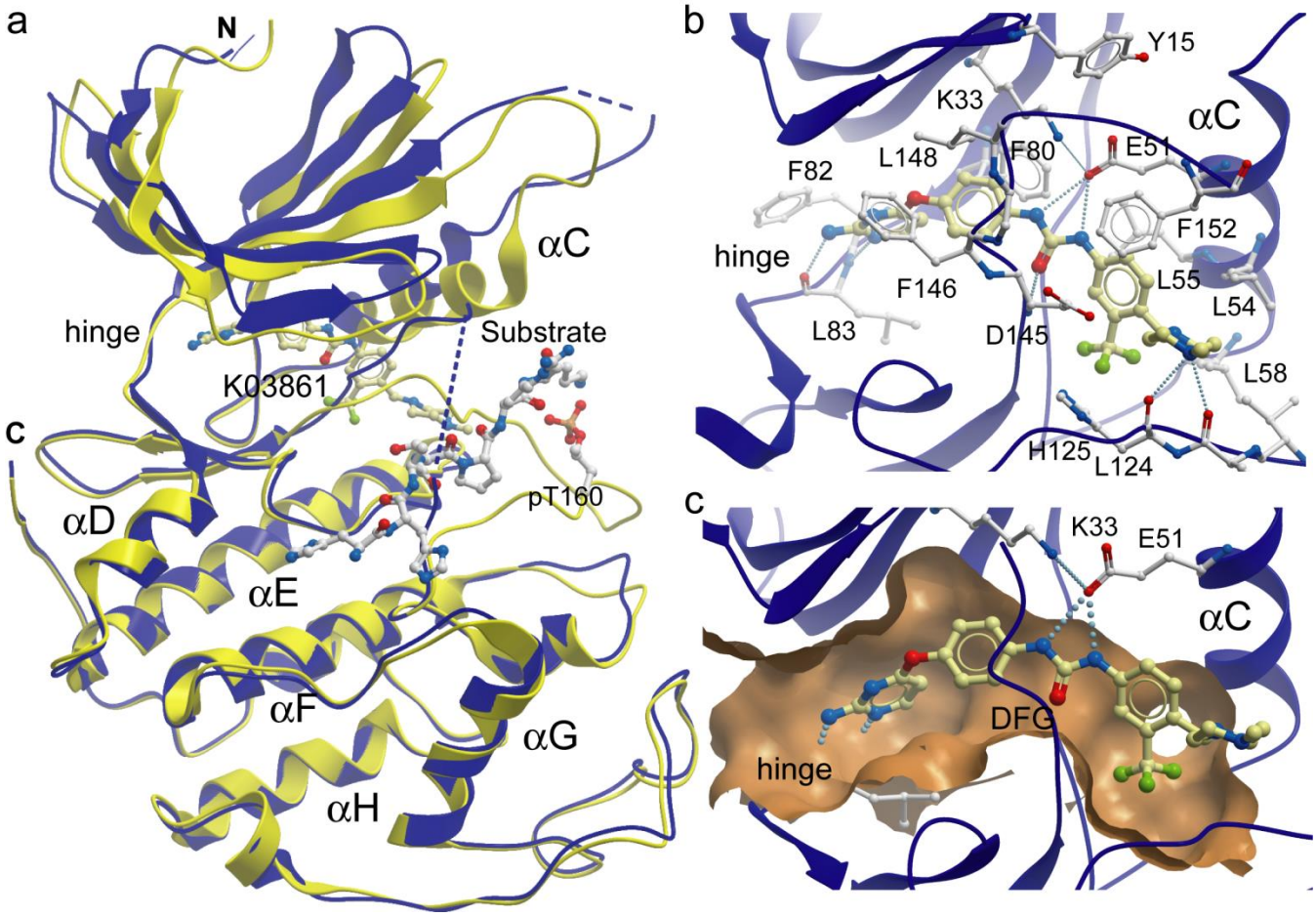

Figure 7. Crystal structure of CDK2 in complex with 1 determined by X-ray crystallography confirms that inhibitor binding occurs to the DFG-out conformation of the kinase. (a) An overlay of the DFG-in (yellow, PDB: 1b38) and DFG-out (blue) CDK2 structures. Large translocation of the DFG-Phe (F146, highlighted) is revealed, while the activation loop of the DFG-in structure is colored in red and the αC helix is in orange. (b) Two typical hydrogen bonds formed with the CDK2 hinge. (c) Hydrogen bond network formed between urea linker, catalytic lysine (K33) and αC-Glu (E51).

Hence, the prolonged compound residence time could be important for its pharmacological selectivity and efficacy, and compounds with a very slow dissociation could have a significant clinical advantage over rapidly reversible inhibitors since they inhibit the activity of a kinase for a significant time period.

The gatekeeper residue and the residue preceding the DFG motif were already pointed out as residues that influence the ability of a kinase to adopt a DFG-out conformation [19]. The authors demonstrated that mutating leucine to cysteine at the DFG-1 position prevents ERK2 from binding to the compound with a type II scaffold, implying that the introduced cysteine disrupts the DFG-out conformation.

This contradicts our results, which suggest that cysteine at this position actually assists in stabilization of the DFG-out state. Moreover, a number of protein kinases that bind type II inhibitors including CDK2 and FLT3 have a cysteine at this position, suggesting that the authors' predictions could be limited to the specific case of that inhibitor probe with ERK2.

However, we demonstrated that similarly to disease-related mutations, amino-acid substitutions can affect dramatically the ability of a kinase to dynamically switch between near-native conformations. Mutations that are located within the active site of CDK2 (A144C), as well as those in the outer interaction shell (C118L), showed a synergistic effect on both catalytic activity of the CDK2 and its ability to bind type II inhibitors.

Our findings support the assumption that a kinase can adopt all major conformations at an energy cost, and further strengthen the concept of a dynamic conformational equilibrium. Essentially, the differences in affinities between the authentic CDK2 and the C118L/A144C mutant imply differences in population of conformers coupled with their inter-conversion rates, and the availability of a DFG-out conformation is the determining factor for the type II inhibition. In the absence of cyclin, the C188L/A144C mutant can more readily form the DFG-out

conformation than the wild-type, which is reflected by more potent binding of the inhibitor **3**.

Upon addition of cyclin, the equilibrium shifted dramatically towards the active DFG-in conformation and therefore binding of this inhibitor to the wild-type could no longer be detected under the same experimental conditions. However, the C118L/A144C mutant still bound type II inhibitors in the presence of cyclin, although affinities of these interactions were significantly reduced compared to those without cyclin. Arguably the introduced point-mutations have only a minor effect, if any, on the overall fold of the kinase or a particular conformational state. This work highlights the importance of conformational adaptation in the evaluation of drug-target interactions. Failure to properly accommodate this may mislead screening campaigns and not only underestimate the affinity and residency time of a compound, but may lead to false negative data for entire compound classes. Unfortunately, the identified inhibitors were promiscuous type II binders precluding mechanistic cell based studies on the cell cycle. Thus, the current type II CDK2 inhibitors will require further optimization in order to obtain more selective compounds in order to compare the effects of the inhibition of inactive CDK2 versus the already well established inhibitors of active CDK2-cyclin complex on the cell cycle and in pre-clinical tumor models.

MATERIALS AND METHODS

Materials: Compounds K03859 (CAS-Nr. 890129-26-7, WO2006059234) and K03861 (CAS-Nr. 853299-07-7, WO2005051366) were kind gifts from Carole Pissot-Soldermann and Andreas Floersheimer (Novartis).

Site-directed mutagenesis: The cDNA sequences available at the Structural Genomics Consortium (SGC) were used as templates for site-directed mutagenesis. All primers used were purchased from Sigma/Aldrich (Oakville, ON). Mutant sequences were generated by site-directed mutagenesis of a wild-type cDNA using the primer extension method [30, 31].

Transformation into *E. coli* protein expression strains: *E.coli* strains of BL21(DE3)-R3-pRARE cells (phage-resistant derivative with a pRARE plasmid encoding rare codon tRNAs) [32] or Rosetta-R3-BirA (encoding the BirA gene for biotin-protein ligase) [33] were used as expression hosts. Competent cells were transformed by heat shock for 45 seconds in a water bath at 42°C, then immediately placed on ice for 2 min, followed by addition of 200 µl LB medium and incubation for 1 hour at 37°C. 50-100 µl transformed cells were plated onto LB-agar media, supplemented with appropriate antibiotics.

Protein expression in *E. coli*: The expression culture was grown in lysogeny broth (LB, Miller) medium at 37°C until OD_{600} of 0.8 was reached. At this point the temperature was reduced to 18°C and expression was induced by the addition of 0.5 mM isopropyl 1-thio-β-D-galactopyranoside (IPTG). Expression was continued for 16 to 18 h. The cells were harvested by centrifugation at 4000g for 20 min at 4°C and re-suspended in lysis buffer comprising 50 mM HEPES pH 7.5, 300 mM NaCl, 5 mM imidazole, 5% glycerol, and 0.5 mM tris(2-carboxyethyl)phosphine (TCEP).

Protein expression in baculovirus-infected insect cells: Insect cell expression systems for CDK2 were used as described [34, 35]. The baculovirus was amplified in *Spodoptera frugiperda* (Sf9) insect cells in Sf900 II media (Invitrogen) and used to infect Sf9 cells grown in suspension to a density of 2×10^6 cells/ml. At 48 h post-infection the cells were harvested by centrifugation at 800*g* for 20 min at 4°C and cell pellets were stored at –20 °C. Cells were re-suspended in a buffer consisting of 10 mM TRIS pH 7.4 and 25 mM NaCl.

Protein purification: The cell suspension was lysed using high-pressure cell homogenization (Avestin C3 Emulsiflex) and cleared by centrifugation at 56.000g for 40 min at 4 °C. The cleared cell lysate was loaded onto a column containing IMAC Sephorose Fast Flow resin (GE Healthcare) equilibrated with lysis buffer. The column was then washed with buffer typically consisting of 50 mM HEPES pH 7.5, 300 mM NaCl, 40 mM imidazole, 5% glycerol and 0.5 mM TCEP. Proteins were eluted with 50 mM HEPES pH 7.5, 300 mM NaCl, 250 mM imidazole, 5% glycerol and 0.5 mM TCEP. The eluted proteins were treated with tobacco etch virus (TEV) protease for 18 h at 4°C (1:20 mass ratio) to remove the hexa-histidine tag, leaving an additional serine residue at the N terminus. The proteins were further purified by size exclusion chromatography by using a Superdex S200 16/60 column (GE Healthcare) buffered in 50 mM HEPES pH 7.5, 300 mM NaCl, 5% glycerol, and 0.5 mM TCEP, at a flow rate of 1 ml/min.

For purification of the untagged protein from insect cell expression, cell extracts were clarified by centrifugation and DNA was removed using a diethylaminoethyl cellulose (DE52, Whatmann) column. The cleared lysate was loaded onto a 5-ml HiTrap Q HP ion-exchange column (GE Healthcare) that was previously equilibrated with buffer containing 10 mM TRIS pH 7.4 and 25 mM NaCl. The flow-through contained the protein, whereas impurities were retarded by the column. The flow-through was subsequently loaded onto 5 ml HiTrap™ Blue HP column (GE Healthcare), and eluted using a linear gradient of up to 1M NaCl. The positive fractions were pooled and dialyzed against 10mM HEPES, pH 7.4, 25mM NaCl, and 5mM DTT.

All protein samples were analyzed by SDS-PAGE (Bio-Rad or Novex) and were concentrated using Amicon-Ultra centrifugal concentrators (Millipore) with a molecular weight cut-off of 10 or 30 kDa. Electrospray ionization time-of-flight (ESI-TOF) mass spectrometry (Agilent) was used to verify the intact mass of the protein. Protein aliquots were flash frozen in liquid nitrogen and stored at –80°C.

Temperature shift assays: The assays were performed as described previously [36]. Briefly, each protein was buffered in 10 mM HEPES, 500 mM NaCl, pH 7.0 at a final concentration of 2 µM and mixed with SYPRO-Orange (Molecular probes, 1000x concentrated stock). Ligands were added at a final concentration of 10 µM. The samples were placed in a 96-well plate, heated from 25 °C to 96 °C at 3 °C per minute and fluorescence levels were recorded at each step by a Stratagene Mx3005P real-time PCR instrument. The change in fluorescence was monitored using excitation and emission filters set to 465 and 590 nm respectively.

Enzymatic assays: A microfluidic electrophoretic mobility-shift assay was used to determine activities of the kinases, observe the effects of mutations and establish kinetic parameters of binding. The assay is based on the electrophoretic separation of phosphorylated (product) and non-phosphorylated (substrate) peptides based on their charge difference [37]. The peptides are tagged with fluorescent marker and the shift in mobility was detected via laser-induced fluorescence allowing for direct and real-time measurements of kinase activities (sequence for CDK2: 5-FAM-QSPKKG-$CONH_2$). Results were expressed as a conversion ratio by measuring peak heights for both the substrate and product and dividing the product peak height by the sum of peak heights for both substrate and product.

Concentrations for the enzyme and ATP were assay specific and optimized for each kinase individually during assay optimization. The assay optimization started with determination of the lowest protein concentration that provides sufficient signal for analysis under conditions of saturating peptide and ATP. This was done to ensure a steady linear reaction with substrate consumption less than 20% so that the initial enzymatic velocity (V) follows the Michaelis-Menten equation. Next, the apparent Michaelis constants for ATP (K_m^{ATP}) and peptide ($K_m^{peptide}$) were obtained from measurements conducted at constant enzyme concentration and a range of ATP and peptide concentrations respectively, and the k_{cat} values were calculated.

For IC_{50} measurements, a 384-well microtiter plate contained 8-point serial dilutions of inhibitors and 16-point serial dilutions of staurosporine as a reference compound. First, 4.5 µl of 2 x kinase solution was added to 0.05 µl compound (maximum concentration 1.8 mM in 90% DMSO and 10% H_2O). To allow for possible slow association, plates with type II inhibitors were incubated for 60 min at 30°C. The assay started after addition of 4.5 µl of 2 x peptide with ATP and was run for 60 min at 30°C, after which 16 µl of stop solution was added (100 mM HEPES pH 7.5, 5% DMSO, 0.1% coating reagent (Caliper Lifescience) 10 mM EDTA pH 8.0, 0.015% BRIJ35). All reactions were performed in 50 mM HEPES, pH 7.5, 1 mM DTT, 0.02% Tween 20, 0.02 % BSA, 10 mM beta-glycerophosphate, 0.01 mM Na_3VO_4, 0.6 % DMSO and 2 µM peptide. Liquid handling and incubation steps were done on a Thermo CatX workstation equipped with Innovadyne Nanodrop Express. Stopped kinase reactions were analyzed using LC3000 or EZ-Reader system (Caliper Life Sciences, Hopkinton, MA, U.S.A.), where both substrate and product were quantified by measuring the laser-induced fluorescence intensities of the peptide's fluorescein labels and calculating the turnover. The dose-dependent influence of the compound on kinase activity was expressed as an IC_{50} value. Each IC_{50} value was calculated from the plot of percentage of inhibition relative to controls versus inhibitor concentration using GraphPad Software or Helios.

Isothermal titration calorimetry: All ITC experiments were performed using a VP-ITC (Microcal, Northampton, MA) instrument at 10°C or 15°C in 50 mM HEPES pH 7.5, 300 mM NaCl and 1 mM DTT and all protein samples were dialysed against this buffer in advance. The concentration of the proteins was between 0.1 mM and 0.2 mM, while the ligand was 10 to 15 times less. A typical titration was conducted using an initial injection of 2 µl, followed by 25 identical injections of 10 µl at time intervals of at least 240 s. Thermodynamic parameters were calculated using Origin 7.0 software (OriginLab, Northampton MA) provided with the equipment and in all cases a single binding site model was employed.

Kinetic experiments based on biolayer interferometry: The binding of CDK2 to inhibitors was analyzed on an Octet RED 384 instrument (FortéBio). Each experiment was performed at 25°C using 50 mM TRIS pH 7.5, 300 mM NaCl, 0.005% P20 Tween and 1 mM DTT as buffer. The buffer-equilibrated super streptavidin biosensors (FortéBio) were loaded with 3 µg/ml biotinylated kinase for 300 s, washed in buffer for 300 s, incubated with inhibitors for at least 300 s, followed by washing in buffer for at least 500 s. Typically, small molecule stock solutions were serially diluted (2.5-fold, 8-point serial dilutions) in buffer. The binding data were fitted using the Octet analysis software 7.0, where the association and dissociation curves were corrected for non-specific binding by subtracting two references: sensors with no kinase incubated with inhibitors and sensors with kinase incubated in buffer.

Crystallization: All crystallization experiments were performed using the sitting drop vapor diffusion method at 4°C in 150 nl drops. CDK2 was buffered in 10 mM Tris-HCl pH7.4, 25 mM NaCl, 5 mM DTT with 1 mM compound added, and concentrated in a 10-kDa-cutoff Amicon Ultra-15 concentrator (Millipore) to 10 mg/ml. Crystals were grown in drops in a reservoir solution containing 10% PEG4000, 0.1 M HEPES pH 7.5 and 0.05 M ammonium sulphate. On mounting, CDK2 crystals were cryo-protected with reservoir solution containing an additional 25% glycerol before transfer to liquid nitrogen.

Structure determination and refinement: Diffraction data were collected at 100 K at the Diamond Light Source. Data processing and refinement were performed

using the CCP4 suite of software [38]. Diffraction images were indexed and integrated using iMOSFLM [39] and data were scaled using SCALA [40]. Phases were calculated by molecular replacement in Phaser [41]. Model rebuilding was carried out using COOT [42] interspersed with cycles of restrained refinement with REFMAC5 [43]. During later stages of refinement, translation/libration/screw (TLS) parameters were introduced. Progress of the refinement for each structure was judged throughout by following a reduction in R_{free} (calculated from 5% of the data that was excluded from the refinement). The stereochemical properties and quality of the final model were assessed with the MOLPBROBITY software [44]. Structural figures and graphical renderings were made with ICM (Molsoft LLC, San Diego, CA).

ASSOCIATED CONTENT

Accession Codes

The structure coordinate of the CDK2-type II inhibitor complexes have been deposited in the Protein Data Bank, ID 5A14.

Supporting Information.

Supplemental figures and tables as described in the text. This material is available free of charge via the Internet at http://pubs.acs.org.

AUTHOR INFORMATION

Corresponding Author

*E-mail: knapp@pharmchem.uni-frankfurt.de; Phone: +49 69 79 82 98 71.

Present Addresses

† ETH Zurich, Institute of Molecular Systems Biology, Auguste-Piccard-Hof 1, 8093 Zurich, Switzerland.

Author Contributions

L.T.A., H.M., S.W.C-J., and S.K. developed the concept, designed experiments and analyzed data. L.T.A. performed experiments. S.K., S.W.C-J., H.M. and S.M.D supervised the project. P.D. provided technical supervision of enzymatic studies and assisted in the design and analysis of these. P.S. contributed to the site-directed mutagenesis and protein purification experiments. O.F. assisted with performing kinetic experiments and provided advice. J.M.E. helped in crystal structure solution. L.T.A. and S.K. wrote the paper. All authors discussed the results and implications and commented on the manuscript at all stages.

Funding Sources

This work was jointly funded by Novartis and EPSRC grant for the SABS IDC. The SGC is a registered charity (No. 1097737) that receives funds from AbbVie, Bayer, Boehringer Ingelheim, Genome Canada through Ontario Genomics Institute Grant OGI-055, GlaxoSmithKline, Janssen, Lilly Canada, the Novartis Research Foundation, the Ontario Ministry of Economic Development and Innovation, Pfizer, Takeda, and Wellcome Trust Grant 092809/Z/10/Z.

Notes

The authors declare no competing financial interest.

ACKNOWLEDGMENT

We would like to acknowledge the support of the members of the SGC Oxford and the Novartis profiling platform. We thank Diamond Light Source for beamtime (proposal mx442).

ABBREVIATIONS

DFG Asp-Phe-Gly motif; CDK cyclin-dependent kinase; ATP ; ITC isothermal titration calorimetry; WT wild type; SEC size exclusion chromatography; SGC structural genomics consortium.

REFERENCES

(1) Liu, Y., and Gray, N. (2006) Rational design of inhibitors that bind to inactive kinase conformations, Nature Chemical Biology 2, 358-364.

(2) Zhao, Z., Wu, H., Wang, L., Liu, Y., Knapp, S., Liu, Q., and Gray, N. (2014) Exploration of Type II Binding Mode: A Privileged Approach for Kinase Inhibitor Focused Drug Discovery?, ACS Chem. Biol. 9, 1230-1241.

(3) Chaikuad, A., Tacconi, Zimmer, J., Liang, Y., Gray, N., Tarsounas, M., and Knapp, S. (2014) A unique inhibitor binding site in ERK1/2 is associated with slow binding kinetics, Nat Chem Biol 10, 853-860.

(4) Noble, M., Endicott, J., and Johnson, L. (2004) Protein Kinase Inhibitors: Insights into Drug Design from Structure, Science 303, 1800-1805.

(5) Hubbard, S. R., Wei, L., Ellis, L., and Hendrickson, W. A. (1994) Crystal structure of the tyrosine kinase domain of the human insulin receptor, Nature 372, 746-754.

(6) Schindler, T., Bornmann, W., Pellicena, P., Miller, W. T., Clarkson, B., and Kuriyan, J. (2000) Structural mechanism for STI-571 inhibition of abelson tyrosine kinase, Science. 289, 1938-1942.

(7) Kufareva, I., and Abagyan, R. (2008) Type-II kinase inhibitor docking, screening, and profiling using modified structures of active kinase states, Journal of medicinal chemistry 51, 7921-7932.

(8) Hasegawa, M., Nishigaki, N., Washio, Y., Kano, K., Harris, P., Sato, H., Mori, I., West, R., Shibahara, M., Toyoda, H., Wang, L., Nolte, R., Veal, J., and Cheung, M. (2007) Discovery of novel benzimidazoles as potent inhibitors of TIE-2 and VEGFR-2 tyrosine kinase receptors, Journal of medicinal chemistry 50, 4453-4470.

(9) Hodous, B., Geuns-Meyer, S., Hughes, P., Albrecht, B., Bellon, S., Caenepeel, S., Cee, V., Chaffee, S., Emery, M., Fretland, J., Gallant, P., Gu, Y., Johnson, R., Kim, J., Long, A., Morrison, M., Olivieri, P., Patel, V., Polverino, A., Rose, P., Wang, L., and Zhao, H. (2007) Synthesis, structural analysis, and SAR studies of triazine derivatives as potent, selective Tie-2 inhibitors, Bioorganic & medicinal chemistry letters 17, 2886-2889.

(10) Tamborini, E., Bonadiman, L., Greco, A., Albertini, V., Negri, T., Gronchi, A., Bertulli, R., Colecchia, M., Casali, P., Pierotti, M., and Pilotti, S. (2004) A new mutation in the KIT ATP pocket causes acquired resistance to imatinib in a gastrointestinal stromal tumor patient, Gastroenterology 127, 294-299.

(11) Kobayashi, S., Boggon, T., Dayaram, T., Jänne, P., Kocher, O., Meyerson, M., Johnson, B., Eck, M., Tenen, D., and Halmos, B. (2005) EGFR mutation and resistance of non-small-cell lung cancer to gefitinib, The New England journal of medicine 352, 786-792.

(12) Azam, M., Seeliger, M., Gray, N., Kuriyan, J., and Daley, G. (2008) Activation of tyrosine kinases by mutation of the gatekeeper threonine, Nature Structural & Molecular Biology 15, 1109-1118.

(13) Quintas-Cardama, A., Tong, W., Manshouri, T., Vega, F., Lennon, P. A., Cools, J., Gilliland, D. G., Lee, F., Cortes, J., Kantarjian, H., and Garcia-Manero, G. (2008) Activity of tyrosine kinase inhibitors against human NUP214-ABL1-positive T cell malignancies, Leukemia 22, 1117-1124.

(14) Emrick, M., Lee, T., Starkey, P., Mumby, M., Resing, K., and Ahn, N. (2006) The gatekeeper residue controls autoactivation of ERK2 via a pathway of intramolecular connectivity, Proceedings of the National Academy of Sciences of the United States of America 103, 18101-18106.

(15) Griffith, J., Black, J., Faerman, C., Swenson, L., Wynn, M., Lu, F., Lippke, J., and Saxena, K. (2004) The structural basis for autoinhibition of FLT3 by the juxtamembrane domain, Molecular cell 13, 169-178.

(16) Wang, Z., Harkins, P. C., Ulevitch, R. J., Han, J., Cobb, M. H., and Goldsmith, E. J. (1997) The structure of mitogen-activated protein kinase p38 at 2.1-A resolution, Proceedings of the National Academy of Sciences of the United States of America 94, 2327-2332.

(17) Shan, Y., Seeliger, M., Eastwood, M., Frank, F., Xu, H., Morten, Dror, R., Kuriyan, J., and Shaw, D. (2009) A conserved protonation-dependent switch controls drug binding in the Abl kinase, Proceedings of the National Academy of Sciences 106, 139-144.

(18) Martin, M., Zhu, J.-Y., Lawrence, H., Pireddu, R., Luo, Y., Alam, R., Ozcan, S., Sebti, S., Lawrence, N., and Schönbrunn, E. (2012) A Novel Mechanism by Which Small Molecule Inhibitors Induce the DFG Flip in Aurora A, ACS Chemical Biology 7, 698-706.

(19) Hari, S., Merritt, E., and Maly, D. (2013) Sequence determinants of a specific inactive protein kinase conformation, Chemistry & Biology 20, 806-815.

(20) Atwell, S., Adams, J., Badger, J., Buchanan, M., Feil, I., Froning, K., Gao, X., Hendle, J., Keegan, K., Leon, B., Müller-Dieckmann, H., Nienaber, V., Noland, B., Post, K., Rajashankar, K. R., Ramos, A., Russell, M., Burley, S., and Buchanan, S. (2004) A novel mode of Gleevec binding is revealed by the structure of spleen tyrosine kinase, The Journal of biological chemistry 279, 55827-55832.

(21) Zuccotto, F., Ardini, E., Casale, E., and Angiolini, M. (2010) Through the "gatekeeper door": exploiting the active kinase conformation, Journal of medicinal chemistry 53, 2681-2694.

(22) Johnson, L. (2009) Protein kinase inhibitors: contributions from structure to clinical compounds, Quarterly Reviews of Biophysics 42, 1-40.

(23) Möbitz, H. (2015) The ABC of protein kinase conformations, Biochimica et biophysica acta.

(24) Garske, A. L., Peters, U., Cortesi, A. T., Perez, J. L., and Shokat, K. M. (2011) Chemical genetic strategy for targeting protein kinases based on covalent complementarity, Proc Natl Acad Sci U S A 108, 15046-15052.

(25) Salonen, L., Ellermann, M., and Diederich, F. (2011) Aromatic Rings in Chemical and Biological Recognition: Energetics and Structures, Angew. Chem. Int. Ed. 50, 4808-4842.

(26) Chakrabarti, P., and Bhattacharyya, R. (2007) Geometry of nonbonded interactions involving planar groups in proteins, Progress in Biophysics and Molecular Biology 95, 83-137.

(27) Kornev, A., and Taylor, S. (2010) Defining the conserved internal architecture of a protein kinase, Biochimica et biophysica acta 1804, 440-444.

(28) Wood, E., Truesdale, A., McDonald, O., Yuan, D., Hassell, A., Dickerson, S., Ellis, B., Pennisi, C., Horne, E., Lackey, K., Alligood, K., Rusnak, D., Gilmer, T., and Shewchuk, L. (2004) A Unique Structure for Epidermal Growth Factor Receptor Bound to GW572016 (Lapatinib), Cancer Research 64, 6652-6659.

(29) Eswaran, J., Bernad, A., Ligos, J., Guinea, B., Debreczeni, J., Sobott, F., Parker, S., Najmanovich, R., Turk, B., and Knapp, S. (2008) Structure of the human protein kinase MPSK1 reveals an atypical activation loop architecture, Structure (London, England : 1993) 16, 115-124.

(30) Reikofski, J., and Tao, B. Y. (1992) Polymerase chain reaction (PCR) techniques for site-directed mutagenesis, Biotechnology advances 10, 535-547.

(31) Heckman, K., and Pease, L. (2007) Gene splicing and mutagenesis by PCR-driven overlap extension, Nat. Protocols 2, 924-932.

(32) Savitsky, P., Bray, J., Cooper, C., Marsden, B., Mahajan, P., Burgess-Brown, N., and Gileadi, O. (2010) High-throughput production of human proteins for crystallization: the SGC experience, Journal of structural biology 172, 3-13.

(33) Keates, T., Cooper, C., Savitsky, P., Allerston, C., Phillips, C., Hammarström, M., Daga, N., Berridge, G., Mahajan, P., Burgess-Brown, N., Müller, S., Gräslund, S., and Gileadi, O. (2012) Expressing the human proteome for affinity proteomics: optimising expression of soluble protein domains and in vivo biotinylation, New biotechnology 29, 515-525.

(34) Rosenblatt, J., De Bondt, H., Jancarik, J., Morgan, D., and Kim, S.-H. (1993) Purification and Crystallization of Human Cyclin-dependent Kinase 2, Journal of Molecular Biology 230, 1317-1319.

(35) De Bondt, H., Rosenblatt, J., Jancarik, J., Jones, H., Morgant, D., and Kim, S.-H. (1993) Crystal structure of cyclin-dependent kinase 2, Nature 363, 595-602.

(36) Fedorov, O., Niesen, F., and Knapp, S. (2012) Kinase inhibitor selectivity profiling using differential scanning fluorimetry, Methods in molecular biology (Clifton, N.J.) 795, 109-118.

(37) Perrin, D., Frémaux, C., and Shutes, A. (2010) Capillary microfluidic electrophoretic mobility shift assays: application to enzymatic assays in drug discovery, Expert Opinion on Drug Discovery 5, 51-63.

(38) (1994) The CCP4 suite: programs for protein crystallography, Acta crystallographica. Section D, Biological crystallography 50, 760-763.

(39) Battye, G., Kontogiannis, L., Johnson, O., Powell, H., and Leslie, A. (2011) iMOSFLM: a new graphical interface for diffraction-image processing with MOSFLM, Acta crystallographica. Section D, Biological crystallography 67, 271-281.

(40) Evans, P. (2006) Scaling and assessment of data quality, Acta crystallographica. Section D, Biological crystallography 62, 72-82.

(41) McCoy, A., Grosse-Kunstleve, R., Adams, P., Winn, M., Storoni, L., and Read, R. (2007) Phaser crystallographic software, Journal of applied crystallography 40, 658-674.

(42) Emsley, P., Lohkamp, B., Scott, W. G., and Cowtan, K. (2010) Features and development of Coot, Acta Crystallographica Section D 66, 486-501.

(43) Murshudov, G. N., Vagin, A. A., and Dodson, E. J. (1997) Refinement of macromolecular structures by the maximum-

likelihood method, Acta crystallographica. Section D, Biological crystallography 53, 240-255.

(44) Davis, I., Leaver-Fay, A., Chen, V., Block, J., Kapral, G., Wang, X., Murray, L., Arendall, B., Snoeyink, J., Richardson, J., and Richardson, D. (2007) MolProbity: all-atom contacts and structure validation for proteins and nucleic acids, Nucleic Acids Research 35, W375-W383.

Insert Table of Contents artwork here